energies

MDPI

Article

A Novel Method for Obtaining the Signature of Household Consumer Pairs

Dadiana-Valeria Căiman * and Toma-Leonida Dragomir

Faculty of Automation and Applied Informatics, Politehnica University Timișoara, 300223 Timișoara, Romania; toma.dragomir@upt.ro

* Correspondence: dadiana.caiman@upt.ro

Received: 23 October 2020; Accepted: 16 November 2020; Published: 18 November 2020

Abstract: The management of electricity consumption by household consumers requires multiple ways of consumer monitoring. One of these is the signature $i(v)$ determined by monitoring the consumer voltage-current trajectory. The paper proposes a novel method for obtaining signatures of 2-multiple consumers, i.e., a pair of consumers connected in parallel. Signatures are obtained from samples of the voltage at the consumers' terminals and of the total current absorbed by the consumers, measured at a frequency of only 20 Hz. Within the method, signatures are calculated using genetic algorithms (GA) and nonlinear regression, according to a procedure developed by the authors in a previous paper. The management of the data selected for the signature assignment represents the novelty. The method proposed in this paper is applied in two case studies, one concerning household consumers within the same power level, the other for household consumers of different power levels. The results confirm the possibility of obtaining signatures of $i(v)$ type.

Keywords: voltage-current trajectory; signatures of household consumers; low frequency sampling with smart meter; nonlinear regression; genetic algorithms; nonintrusive decomposition of compound consumers via signatures

1. Introduction

Domestic consumption of electricity is increasing year after year, both by the diversity of household appliances and by their number. A useful step in the reduction or the management of consumption as well as in the detection of events is the automatic generation of consumption maps, based on the identification of the consumers' characteristics, including the household consumers. The results can be used to generate consumption predictions with various applicability: energy saving [1], grid balancing by eliminating consumption peaks [2,3], local management of green energy sources [2,3], as well as detecting atypical behaviors that may be due to device failure [4], power theft [5], etc. In this context, the concept of signature was promoted. The signature of a consumer or a group of consumers, hereinafter referred to as a multiple consumer (m_c), is defined as a characteristic or set of customized power characteristics enabling the single consumer or the multiple consumer to be uniquely identified.

When aiming to identify the signature in a nonintrusive manner with the help of smart power meters, the choice of power characteristics used as a signature depends on the meters' features. The issue of signature-based identification of devices was, to our knowledge, first raised by Hart [6]. The power characteristic taken into account was the admittance in the complex space of normalized power, under permanent regime, and the purpose of the signature was to group similar devices allowing further clustering analysis. Today the signature composition is oriented towards power characteristics specific to stabilized and/or transient regimes that require a high data acquisition frequency. All methods are empirical in nature.

Three steps are taken in identifying consumers in general: the detection of an event, the recording of the power characteristics involved in defining the signature and the application of the classification/identification algorithm. Identification/classification algorithms are generally the algorithms of supervised deep learning and unsupervised deep learning algorithms. The first category, unlike the second one, requires pretraining using a labelled data set.

In this article the identifying of consumers is done by using the voltage-current signature "V-I", widely referenced in the literature.

The concept appears for the first time in [7], Lam associating the signature to a set of eight geometric identifiers of the V-I trajectory. The aim is to cluster consumers by the hierarchical clustering method.

Subsequently, in [8], Hassan uses six of the identifiers introduced by Lam as well as an additional identifier called span and defined as the difference between the maximum and minimum value of the V-I trajectory. Due to its proportionality to the active power, the span is used for event detection. The classification algorithms applied are feed-forward artificial neural network, artificial neural network + evolutionary algorithm, support vector method, and Adaptive Boost.

In [9], Wang considers as electrical features: the geometrical identifiers proposed by Lam, the span introduced by Hassan and the variation of instant admittance. He uses reactive power variation to detect an event. The support vector machine algorithm is proposed as identification algorithm. The identification rate is very good for an acquisition frequency in the range of 9–18 kHz and drops steeply for values below 2 kHz.

In [10], Iksan uses a hybrid set of features consisting of two geometric characteristics associated to the V-I trajectory, total harmonic distortion and phase shifting as a signature having 91% accuracy. The clustering method used is hierarchical clustering.

Another way of approaching the problem is to map the V-I trajectory in a binary matrix. In [11], Du proposes a classification into seven categories of consumers based on the V-I trajectories and a set of six characteristics derived from the binary image (specific values for certain cells/sets of cells in the binary matrix, two cells and three columns are actually used) which build signatures by combination. The supervised self-organization map is used as an identification/classification algorithm.

In [12], Baets considers weighted pixilated V-I image (gray image) as a signature. Signature building has as its first step the trajectory mapping in a binary matrix, for each cell of the binary matrix retaining the number of points in the trajectory that it includes. The convolutional neural network (CNN) is used as classification algorithm. In [13], the same author aims to detect several household consumers whose signatures were not included in the initial implementation of the classification/identification algorithm. In this case, the binary image of the voltage-current trajectory is considered the signature. The density-based spatial clustering algorithm is used in the classification to determine outliers equated with unknown consumers.

The CNN algorithm is used by Faustine in [14,15]. In both papers a weighted recurrent graph, based on Euclidean distance similarity function, is used to map one-cycle current into an 'colored' image. In [14], the event detection underlies the classification. An interesting approach emerges in [15] where Faustine applies the CNN to one-cycle of nonactive current (Fryze-current decomposition) that contains more than one appliance.

In [16], Baptista uses the same classification algorithm and the image of V-I trajectory as signature.

In [17], the image of the V-I trajectory is reduced using an image pyramid reduction algorithm, taking into account only quadrants 1 and 3 of the representation (working with inductive and resistive consumers). The classification algorithm is based on the main component analysis and k-nearest neighbor algorithm.

A binary trajectory mapping followed by staining with the HSV color space is proposed in [18]. The CNN is used as a classification algorithm, pretested on a data set associated to visual recognition.

In most cases the detection of an event (on/off or the consumer's transition from one state to another) is based on the changes occurred in power and/or span [8]. As a result, measurements of aggregate power (e.g., at apartment level for domestic consumers) are required to detect consumers'

transitions between states over timeframes. In [13], Baets considers that, in principle, the detection of an event is a side effect of the identification algorithm.

The studies referred to in articles [19–21] were triggered by the fact that signatures are obtained by sampling currents, voltages, and powers at frequencies of thousands of Hz, using methods that go beyond the capabilities of current meters. In the experiments the sampling was performed with a frequency of approx. 20 Hz, compatible with the capabilities of meters available on the market. The results obtained relate to consumers such as laptops, vacuum cleaners, televisions, etc. In these papers, like in the others mentioned above, the topic of determining the signature was limited to simple consumers or equivalent consumers. In this context, investigating the possibility of obtaining individual signatures from global consumption, i.e., from the total consumption of a multiple consumer, is, of course, a challenge. As the experimental data obtained from simple and multiple consumers are of the same type, a new method of investigation that is capable of discrimination was needed for multiple consumers.

Throughout the article we refer to an assembly of n household appliances connected in parallel to a shared power source, appliances that are in the "on" mode of operation at any given moment as a n-multiple consumer (*n-m_c*). If n = 1, we are referring to as a simple consumer. When an *n-m_c* is approximated as simple consumer, we are referring to as equivalent simple consumer (*e-s_c*).

In this paper the authors aim to develop a signature allocation method for 2-*m_c* based on an acquired data set with a frequency of only 20 Hz [19]. The method does not involve the explicit use of a detection algorithm within the purposes of the work [8]. Signature is formed by associating an analytical function, called "V-I trajectory support function" having a set of parameters. The set of parameters is calculated using GA. Other calculation tools can be used.

Further down the presentation is structured as follows: Section 2 summarizes how to identify a simple consumer and introduces the terminology used in the rest of the paper. Section 3 shows the method of obtaining the signature of a 2-*m_c*. It uses tools used by authors in [20,21]. Section 4 presents two case studies. Finally, Section 5 summarizes the conclusions and possible subsequent directions of research.

2. Selecting the Subsets of Points for Assigning the Signature

The identity of a simple consumer can be expressed by various means. One of them is the V-I trajectory, i.e., the dependence $i(v)$ between the voltage v at the consumer's terminals and the absorbed current i. The dependency links the values of the current i and of the voltage v at the moment t [7]. The voltage range is $[V_{min}, V_{\max}]$.

In [21], a method is presented to obtain the signature $i(v)$ of a simple consumer from a set of values pairs $\{v(t), i(t)\}$, taken in discrete time. The method is based on the setup of a selected $S_k(v)$ support function from the four support functions specified in Appendix A, associated with a group of four classes of consumers $k \in K$, $K = \{1, \ldots, 4\}$: $k = 1$—tangent class, $k = 2$—discontinuous tangent class, $k = 3$—ellipse class, and $k = 4$—hybrid class. The hybrid class has the widest area of coverage in applications. The nonlinear regression sets up the support functions by using GA. The method undergoes three steps:

1. Selecting the subsets of points used to assign the signature;
2. Associating the support function, choosing the fitness function, and setting up the support function for each branch separately, by nonlinear regression using GA;
3. Validation of the solution calculated based on physical considerations.

In addition to those presented in [21], the following aspects of step 1 are important in the following.

In the ideal case the voltage of the network is sinusoidal of 50 Hz, and for time-invariant consumers the trajectories $i(v)$ are closed curves, due to periodicity. The curves have two branches: an ascending branch (a) corresponding to the time intervals during which $v(t)$ increases from V_{min} to V_{max}, and a descending branch (d), corresponding to the time intervals during which $v(t)$ decreases from V_{max} to

V_{min}. In real cases, $v(t)$ is not purely sinusoidal and the consumers are actually not time-invariant. Consequently, the actual trajectories $i(v)$ show dispersed deviations by reference to the ideal trajectories. Further, we refer to the branch index as r; therefore $r \in \{a, d\}$.

The study in this paper, like the study in [21], was carried out under the real conditions stated above. The value pairs $\{(v(t), i(t))\}$ were extracted with a frequency of approx. 20 Hz within a time span of approx. 1 min. Due to the low value of extraction frequency and due to disturbances that affected the measurements, the dispersion level of the selected points set has increased in comparison to an ideal trajectory.

The graphic aspect of the measured values is a "point cloud". Figure 1a exemplifies a measured point cloud of 1024 points $\{(v(t), i(t))\}$. The cloud highlights an $i(v)$ trajectory with two non-intercrossing branches, an ascending one (lower curve) and a descending branch (upper curve), with common points at the extremities. In Figure 1b, an image of the same point cloud joined with straight segments in the sequence in which they were extracted is presented. As two successive points correspond to moments with about 2.5 periods of network voltage distance, often one on an ascending branch and the other on a descending branch, the resulting figure has the appearance of a continuum. This representation suggests the possibility that the two branches may intersect. For simple consumers analyzed in [21] the branches did not intersect.

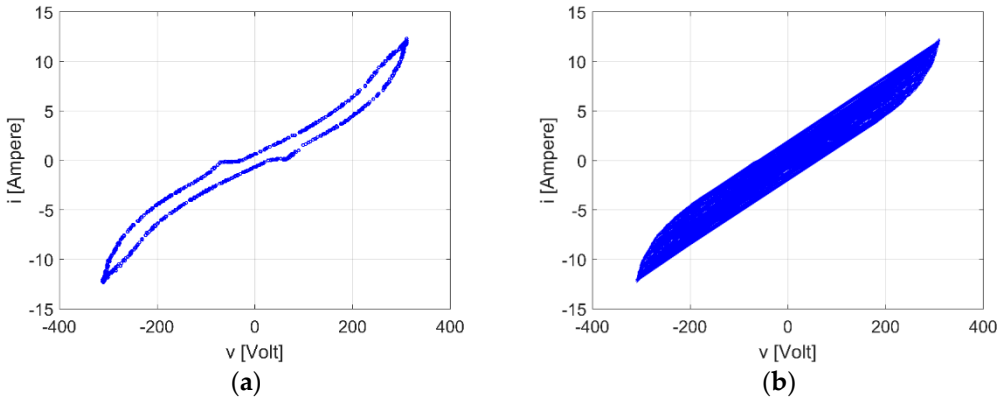

Figure 1. Images of a point cloud resulting from measurements: isolated points (**a**), points joined with straight segments (**b**).

The selection of the subsets of points used to assign signatures is the operation by which two subsets of points, M_a and M_d, are selected from the initial point cloud and then used to identify the signature branches. The selection method adopted in [20], also used in this case, is essentially a filtration process which introduces deviations from the ideal situation.

3. Determining the Signatures of a N-Multiple Consumer

Due to the parallel connection of the n simple consumers, the instantaneous current consumed by a *n-m_c* is the sum of the instantaneous currents consumed by the component consumers, and the points $\{v(t), i(t)\}$ reflect the instantly measured values of the common voltage and the total current consumed i:

$$i(t) = i^1(t) + i^2(t) + \ldots + i^n(t). \quad (1)$$

It is possible to assign several types of voltage-current signatures to an *n-m_c*, unlike the simple consumer. The following variants have practical importance:

- Variant 1: assigning of a single dependence $i(v)$, i.e., an *e-s_c*;
- Variant 2: assigning a number of s dependencies $i(v)$, $(1 < s < n)$, i.e., a set of dominant signatures $i^1 = f_1(v)$, $i^2 = f_2(v)$, ... , $i^s = f_s(v)$, without individualized physical correspondent, but which has as equivalent the entire multiple consumer by summarizing the currents;

- Variant 3: assigning a number of n dependencies $i(v)$, $i^{\lambda} = f_{\lambda}(v)$, $\lambda = 1, \ldots, n$, having in view that each dependency corresponds to one of the n simple consumers forming the *n-m_c*.

In the following sections we extend the research reported in [21] to the case of a 2-*m_c* for which only the versions 1 and 3 make sense, i.e., assigning a single dependence $i(v)$ with signature role for a simple equivalent consumer, respectively assigning a pair of dependencies $\{i^1 = f_1(v), i^2 = f_2(v)\}$. In the second case, it is normal to consider whether the dependencies assigned to 2-*m_c* correspond to the signatures of simple real consumers or only to mathematically equivalent consumers. The support functions used in the study belong to the classes listed in Appendix A.

3.1. Signatures Assignment for Variant 1

The assignment of a single equivalent signature shall be carried out according to the method set out in [21], summarized in Section 2. This will result in an approximating signature belonging to one of the four K classes.

3.2. Signatures Assignment for Variant 3

The signature assigning process undergoes four steps:

1. Selecting the subsets of points used to assign the signature;
2. Taking-up the set of pairs of support functions $C_{\alpha\beta} = \{S_{\alpha}(v), S_{\beta}(v)\}$, $\alpha, \beta \in K$, of the weights applied to these, and of the associated fitness functions;
3. Nonlinear regression using GA setting up of the support functions parameters;
4. Determination of the 2-multiple consumer's signature.

Step 1: goes similarly to stage 1 for variant 1.

Step 2: We considered that all the pairs of simple consumers, $C_{\alpha\beta}$, for each r branch are admitted, the index α and β having all values $k \in K$. Therefore, a number of 16 pairs $C_{\alpha\beta}$ of support functions: $\{C_{11}, C_{12}, C_{13}, C_{14}, C_{21}, C_{22}, C_{23}, C_{24}, C_{31}, C_{32}, C_{33}, C_{34}, C_{41}, C_{42}, C_{43}, C_{44}\}$ has resulted for each branch. In order to determine the parameters corresponding to a $C_{\alpha\beta}$ pair and to a r branch, using GA, we applied the fitness functions (2):

$$F_{\alpha\beta\_r\_p} = 1/N_r \cdot \sum_{1}^{N_r} \left[\left| i_j - i_{\alpha\beta\_r\_p}(v_j) \right| \cdot \left(1 + 0.2 \cdot \exp\left(-\left|v_j / V\right|\right)\right) \right] \tag{2}$$

where

$$i_{\alpha\beta\_r\_p}(v_j) = i_r^1(v_j) + i_r^2(v_j) \tag{3a}$$

$$i_r^1(v_j) = p \cdot S_{\alpha}(v_j), i_r^2(v_j) = (1 - p) \cdot S_{\beta}(v_j) \tag{3b}$$

In (2), N_r is the number of points in the M_r set, i_j the measured value of the total absorbed current corresponding to the v_j value of the terminal voltage at the instant t_j, i.e., $i_j = i(v(t_j))$, p the weighting parameter used to calculate the $i_{\alpha\beta\_r\_p}$ value of the total current absorbed, and V an attenuation constant of the measured voltage values. The value $V = 300$ Volt was considered.

The weighting is necessary because (i) the levels of the powers of the simple real consumers who are forming the 2-*m_c* can have different size ranges; (ii) the fitness $F_{\alpha\beta_r_p}$operates with the total current absorbed on each branch. For the general case, we considered that p takes values within the P set:

$$P = \{0.2, 0.4, 0.5, 0.6, 0.8\}. \tag{4}$$

Weighting allows for the values calculated using the supporting functions $S_\alpha(v_j)$ and $S_\beta(v_j)$ to be adjusted evenly throughout the range of voltage variation at the terminals. Hence, the total currents absorbed on the branches (*a*) and (*d*) are:

$$i_{\alpha\beta\_a\_p}(v_j) = p \cdot S_{\alpha\_a}(v_j) + (1-p) \cdot S_{\beta\_a}(v_j), \quad i_{\alpha\beta\_d\_p}(v_j) = p \cdot S_{\alpha\_d}(v_j) + (1-p) \cdot S_{\beta\_d}(v_j), \quad p \in P. \tag{5}$$

The values $S_{\alpha\_r}(v_j)$ and $S_{\beta\_r}(v_j)$ were calculated using the expressions of the support functions listed in Appendix A.

It is important to notice that by considering the *P* set formed according to (4), the $C_{\alpha\beta}$ pair having the parameter *p* and $C_{\beta\alpha}$ pair having the parameter $1 - p$ are leading to the same result. Consequently, the number of analyzed combinations was limited to $q = 10$: $\{C_{11}, C_{12}, C_{13}, C_{14}, C_{22}, C_{23}, C_{24}, C_{33}, C_{34}, C_{44}\}$.

Step III: For each $C_{\alpha\beta}$pair, the support functions related to the ascending branches, $S_{\alpha\_a}(v)$ and $S_{\beta\_a}(v)$, respectively to the descending ones, $S_{\alpha\_d}(v)$ and $S_{\beta\_d}(v)$, are introducing implicitly the parameters sets Π_{α_a} and Π_{β_a}, respectively $\Pi_{\alpha_d}$and Π_{β_d}. The calculation of the pair of signatures corresponding to the *r* branch is considered finalized once the calculation of the pair $\{\Pi_{\alpha\_r}, \Pi_{\beta\_r}\}$ with GA using the set M_r and the fitness $F_{\alpha\beta_r_p}$is done. Taking into consideration the GA's operation mode, each usage of GA for a point cloud M_r, a combination $C_{\alpha\beta}$, and given *p* and *r*, after a sufficiently high number n_G of generations, is resulting in the stabilization at new values of the parameters $\{\Pi_{\alpha\_r}, \Pi_{\beta\_r}\}$, respectively the fitness $F_{\alpha\beta\_r\_p}$. We found out experimentally that the stabilization is achieved after $n_G = 200$ generations.

The operations by which the set of $F_{\alpha\beta\_r\_p}$ values and the values of the parameters set $\{\Pi_{\alpha\_r}, \Pi_{\beta\_r}\}$ are determined simultaneously, but calculated independently, for all the *q* pairs $C_{\alpha\beta}$ is referred to as "independent run". We note the rank number of the independent runs by θ, $\theta = 1, 2, \ldots, m$.

Due to the dispersion of the measuring points within the point cloud M_r and due to the local minima of the support functions, the sequence $\{F_{\alpha\beta\_r\_p\_\theta}\}_{\theta = 1, 2, \ldots, m}$, of fitness corresponding to a $C_{\alpha\beta}$ combination obtained during several independent runs is not constant. The values $F_{\alpha\beta\_r\_p\_\theta}$ differ from an independent run to another. The experimental convergence tests led us to the conclusion that the sequences of values $\{F_{\alpha\beta\_r\_p\_\theta}\}_{\alpha\beta \in C\alpha\beta,\ r \in \{a,\ d\},\ p \in \{0.2,\ 0{,}4,\ 0.5,\ 0{,}6,\ 0{,}8\},\ \theta = 1, 2, \ldots, m}$ are stabilized after a number $m = 50$ independent runs.

In this context we presume that we performed for each *p* weighting, each *r* branch, and for all those $q = 10$ combinations, *m* independent runs, each with the extension of n_G generations. We systematize the 500 results (fitness and parameters of combinations participating in an independent run) as in Table 1 except the last line and the last column. In total, we obtain five tables for $r = a$ and five tables for $r = d$.

Table 1. Fitness and signature parameters for independent runs corresponding to given *p* and *r*.

θ	C_{11}	C_{12}	...	C_{44}	$C^{\theta}_{\alpha\beta}$
1	$F_{11\_r\_p\_1}$, $\Pi_{1\_r\_p\_1}$, $\Pi_{1\_r\_1\text{-}p\_1}$	$F_{12\_r\_p\_1}$, $\Pi_{1\_r\_p\_1}$, $\Pi_{2\_r\_1\text{-}p\_1}$	...	$F_{44\_r\_p\_1}$, $\Pi_{4\_r\_p\_1}$, $\Pi_{4\_r\_1\text{-}p\_1}$	$C^{1}_{\alpha\beta}$
...	...	...	...	...	...
50	$F_{11\_r\_p\_50}$, $\Pi_{1\_r\_p\_50}$, $\Pi_{1\_r\_1\text{-}p\_50}$	$F_{12\_r\_p\_50}$, $\Pi_{1\_r\_p\_50}$, $\Pi_{2\_r\_1\text{-}p\_50}$	...	$F_{44\_r\_p\_50}$, $\Pi_{4\_r\_p\_50}$, $\Pi_{4\_r\_1\text{-}p\_50}$	$C^{50}_{\alpha\beta}$
$f_{p,r}$	$f_{p,r,11}$	$f_{p,r,12}$		$f_{p,r,44}$	f_{pr}

Step 4: For each *r*, there is a minimum fitness among the 2500 fitness values in the five tables of type Table 1. We note it with $F_{r,min}$. This cannot be considered the solution to the problem since the operations that led to the value of $F_{r,min}$ may ignore certain deviations of the related signature from the M_r set. In view of this aspect, we adopted the following procedure for obtaining the solution, i.e., a pair of signatures:

1. In Table 1 we selected in the last column of each row the symbol of the pair with the lowest fitness. Thus, $C^1_{\alpha\beta}$ is the symbol of the $C_{\alpha\beta}$ set from the independent run 1 that corresponds to $\min\{F_{\alpha\beta\_r\_p\_1}\}_{\alpha\beta \in \{11, 12, \dots, 44\}}$, and $C^{50}_{\alpha\beta}$ is the symbol of the $C_{\alpha\beta}$ set that corresponds to the lowest fitness of the run 50, $\min\{F_{\alpha\beta\_r\_p\_50}\}_{\alpha\beta \in \{11, 12, \dots, 44\}}$.
2. The frequencies of all combinations from Table 1 ($f_{p,r,11}$, … , $f_{p,r,44}$) shall be calculated using the Equation (6) and then the maximum score f_{p,r_max} using the Formula (7):

$$f_{p,r,\alpha\beta} = \text{(the number of occurrences of the } C_{\alpha\beta} \text{ combination in the last column of Table 1)/m.} \tag{6}$$

$$f_{p,r\_max} = \max\{f_{p,r,\alpha\beta}\},\ \alpha, \beta \in K. \tag{7}$$

The results are inserted in first row in Table 2. The second row will display the minimum value of the fitness that contributed to the determination of the values in the first row. According to the example of Table 2 the maximum frequency $f_{0.6,r\_max} = 0.66$ corresponds to $p = 0.6$, this frequency occurs for the C_{24} combination having a minimum fitness $F_{0.6,r} = 0.12345678$. We denote by $\{F_{p,r}\}$ the set of all $F_{p,r}$ values from Table 2.

Table 2. The maximum frequencies of the combinations analyzed for the *r* branch and the related minimum fitness.

$f_{0.2,r,\#\#} = \dots$	$f_{0.4,r,\#\#} = \dots$	$f_{0.5,r,\#\#} = \dots$	$f_{0.6,r,24} = 0.66$	$f_{0.2,r,\#\#} = \dots$
$F_{0.2,r} = \dots$	$F_{0.4,r} = \dots$	$F_{0.5,r} = \dots$	$F_{0.6,r} = 0.12345678$	$F_{0.8,r} = \dots$

3. Determining the solution corresponding to branch *r* implies the following steps: we chose the combination $C_{\alpha\beta}$ corresponding to the lowest fitness $F_{p,r}$ according to equation

$$F_r = \min_{p \in P}\left\{F_{p,r}\right\} \tag{8}$$

as the first solution to the problem. Where the partial signatures $i^1_r(v_j)$ and $i^2_r(v_j)$ have a physical meaning, this first solution is adopted as solution of the problem. Otherwise, we proceeded by making a new choice in the ascending order of the fitness in set $\{F_{p,r}\}$.
4. The signatures of the two member consumers of 2-*m_c* are determined by combining the partial signatures of the two branches $i^1_a(v_j)$ and $i^2_a(v_j)$, respectively $i^1_d(v_j)$ and $i^2_d(v_j)$ with formulas of the types (9a) and (9b):

- Consumer 1:

$$i^1(v) = \begin{cases} p \cdot S_{\alpha\_a}(v) \textit{having parameters } \Pi_{\alpha\_a} \textit{for the ascending branch} \\ p \cdot S_{\alpha\_d}(v) \textit{having parameters } \Pi_{\alpha\_d} \textit{for the descending branch} \end{cases} \tag{9a}$$

- Consumer 2:

$$i^2(v) = \begin{cases} (1-p) \cdot S_{\beta\_a}(v) \textit{having parameters } \Pi_{\beta\_a} \textit{ for the ascending branch} \\ (1-p) \cdot S_{\beta\_d}(v) \textit{having parameters } \Pi_{\beta\_d} \textit{ for the descending branch} \end{cases} \tag{9b}$$

4. Case Studies

We consider below to case studies relating to two 2-*m_c*. Their relevance is given by the fact that in the case study 1 (CS1) the consumer consists of two consumers with power levels of the same size range, while case study 2 (CS2) consists of two consumers with power levels of different

sizes. The implementation of the signature determination method was performed using the Matlab environment, version R2016a.

4.1. Case Study No. 1

In CS1 the 2-*m_c* consists of a DELL laptop and an LCD TV with active powers in a ratio of approx. 1/2.3. The laptop represents a consumer of class $k = 1$ and the TV a consumer of class $k = 2$ [21]. The point cloud obtained by measurements and the point sets selected for determining signatures (M_a—blue and M_d—red) are illustrated in Figure 2.

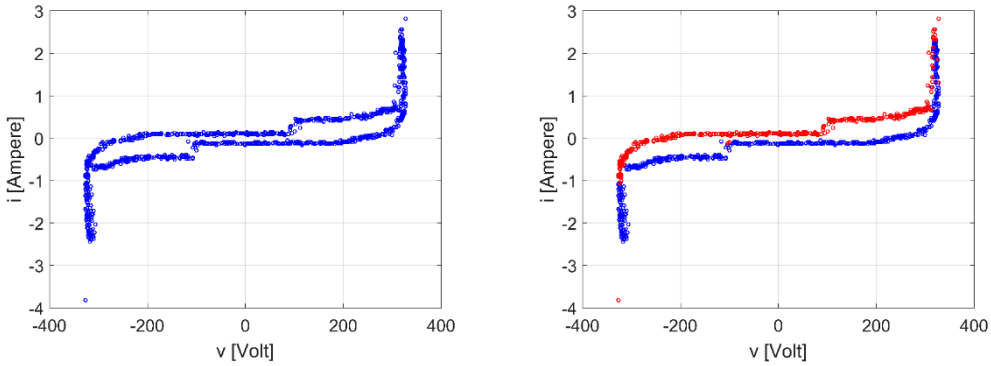

Figure 2. The measured point cloud (**a**) and the sets M_a and M_d (**b**) for CS1.

For variant 1, the fitness corresponding to the four support functions in Appendix A have the values in Table 3. The best results are underlined. They recommend the adoption of a class $k = 4$ *e-s_c* model. The obtained parameters have the values in Appendix B: (B1) for the ascending branch and (B2) for the descending one.

Table 3. The fitness values of the simple equivalent consumers (variant 1) for CS1.

r	$k = 1$	$k = 2$	$k = 3$	$k = 4$
a	0.413636	0.324093	0.714877	0.240222
d	0.205723	0.172016	0.649751	0.095465

The two branches are illustrated both separately and together in Figure 3. The point-sets M_a and M_d are illustrated in blue and the signatures in red.

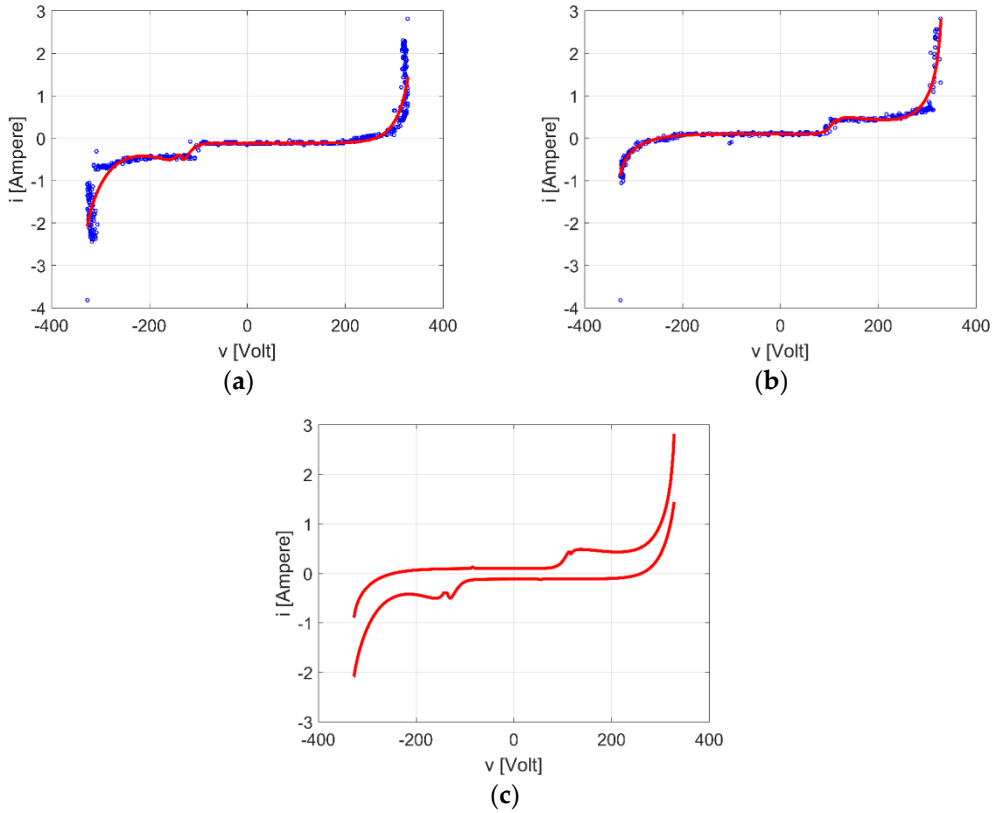

Figure 3. The signature of a *e-s_c* of class $k = 4$ for CS1: ascending branch (**a**), descending branch (**b**), assembly (**c**).

Next we address the problem in the variant 3. The distribution of the maximum frequencies for the 10 combinations corresponding to independent run is listed in Table 4. The underlined values indicate the minimum fitness $F_{a,min}$ and $F_{d,min}$, respectively.

Table 4. CS1—Maximum frequencies of the analyzed combinations for the branches a and d and the associated minimum fitness.

$f_{0.2,a,44} = 0.78$ $F_{0.2,a} = 0.2409420$	$f_{0.4,a,44} = 0.64$ $F_{0.4,a} = 0.239268202$	$f_{0.5,a,44} = 0.56$ $F_{0.5,a} = 0.238015452$	$f_{0.6,a,44} = 0.46$ $F_{0.6,a} = 0.237630446$	$f_{0.8,a,24} = 0.56$ $F_{0.8,a} = \underline{0.219822977}$
$f_{0.2,d,44} = 0.82$ $F_{0.2,d} = 0.09960277$	$f_{0.4,d,44} = 0.58$ $F_{0.4,d} = 0.10052771$	$f_{0.5,d,24} = 0.56$ $F_{0.5,d} = 0.094081329$	$f_{0.6,d,24} = 0.54$ $F_{0.6,d} = 0.102157999$	$f_{0.8,d,24} = 0.56$ $F_{0.8,d} = \underline{0.09077883}$

In the case of the ascending branch we chose for the beginning as a solution the combination with fitness $F_a = 0.219822977$. This is pair C_{24} for $p = 0.8$, identical to pair C_{42} for $p = 0.2$. We noticed that from the set of values $\{p/(1 - p)\}_{p \in P}$, the ratio $0.2/0.8 = 1/4$ has the closest value to the power ratio 1/2.3 originally specified. The choice corresponds to a 2-*m_c* consisting of two simple consumers with $k = 2$ (discontinuous tangent class) and $k = 4$ (hybrid class).

In Figure 4a, the resulting component signatures for the ascending branch are illustrated. The signature parameters of the simple consumers associated with the C_{24} pair have the values of (B3) and (B4). The sum of the two signatures is represented with a red line. Figure 4b shows a very good positioning of the sum in relation to the M_a set of points. With the exception of the area of very high voltage values at terminals v, the signatures validate the calculation performed. The deviation displayed by this area may be explained by the truncation of the number of points that form the M_a set.

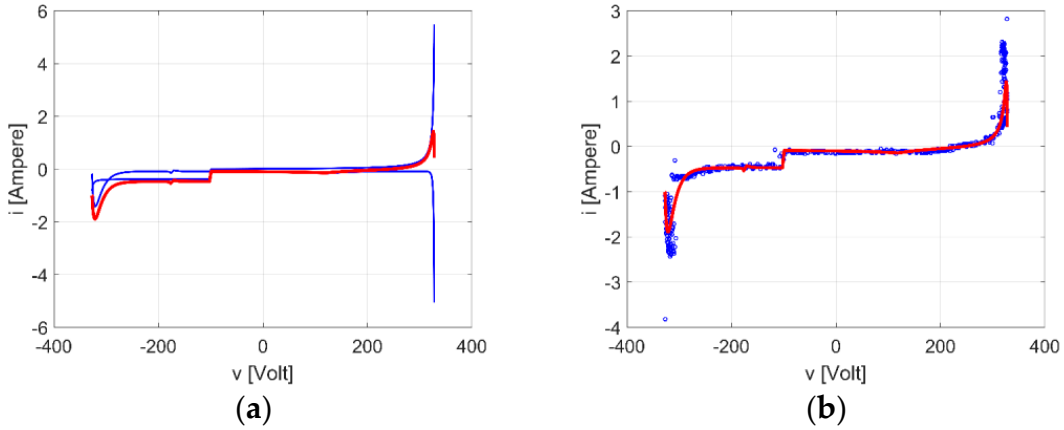

Figure 4. CS1—solution for the ascending branch, the 3rd variant: the branch (red) and its components (blue) (**a**); the branch (red) vs. the *Ma* set of points (blue) (**b**).

It is well known that GA can lead to solutions that converge towards local minima. In this case, they will be removed if the signatures do not have physical sense. We illustrate this by considering, in ascending order, the second value of the second row in Table 4: $F_{0.6,a} = 0.237630446$. It corresponds to pair C_{44}. The signatures appear in Figure 5. Even if the overall results are good (Figure 5a), the solution is not validated because the signature of one of the consumers has only strictly positive values (Figure 5b).

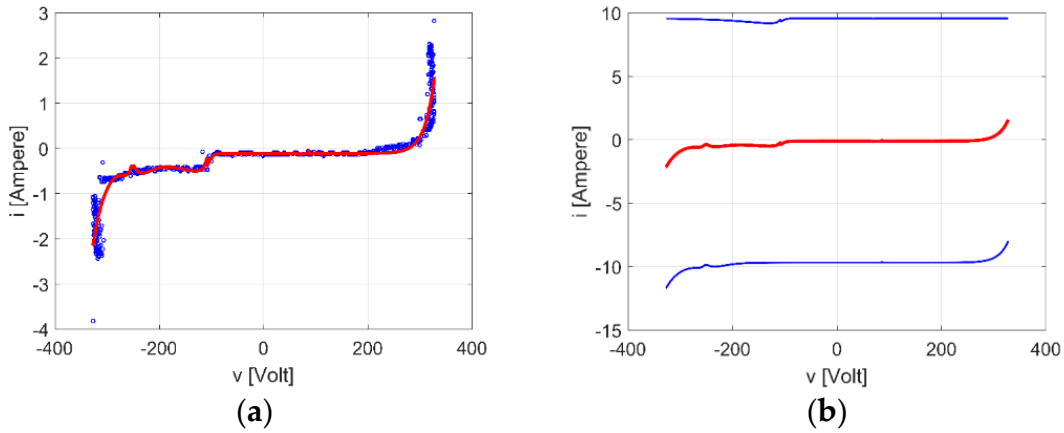

Figure 5. An invalid choice for the ascending branch in CS1, variant 3, $F_{0.6,a} = 0.237630446$: the branch (red) vs. the M_a set of points (blue) (**a**); the branch (red) and its components (blue) (**b**).

For the descending branch, according to the same reasoning, we consider the fitness $F_{0.8,d} = 0.09077883$ (row 3 of Table 4)—corresponding to the pair C_{24}. The signatures shown in Figure 6 validate the result. The values of the parameters of the signatures of simple consumers associated with the C_{24} pair are those in (B5) and (B6).

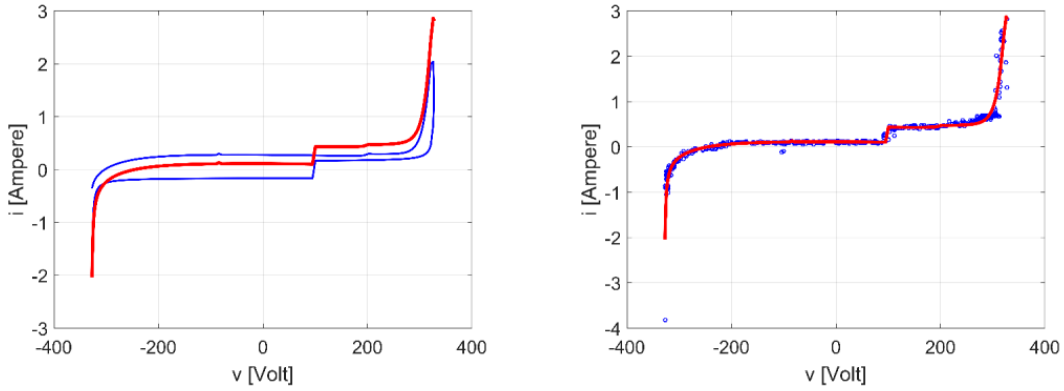

Figure 6. CS1—solution for the descending branch in the 3rd variant, $F_{0.8,d}$ = 0.09077883: the branches (red) and its components (**a**); the sum of the branches vs. the M_d set of points (**b**).

Unlike the ascending branch, this time the next two values in the last row of Table 4 lead to physically valid results. For example, $F_{0.5,d}$ = 0.094081329 corresponds to the signatures in Figure 7.

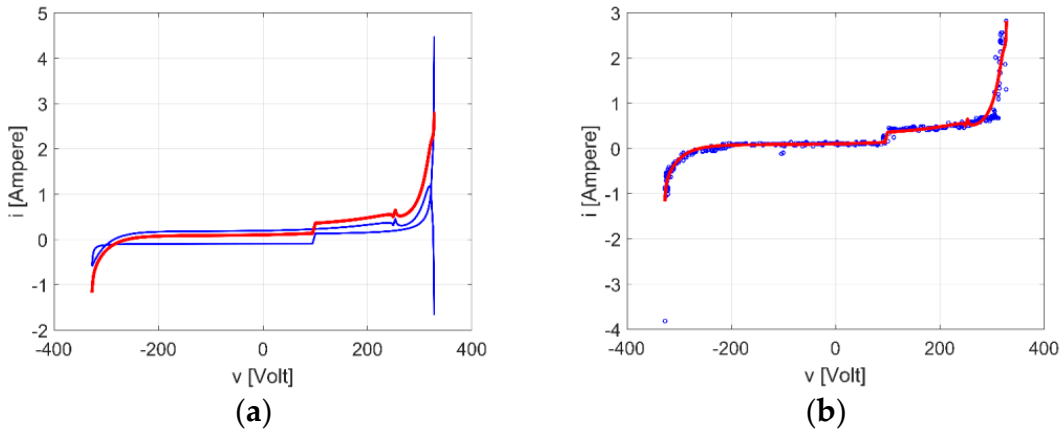

Figure 7. CS1—potential solution for the descending branch, $F_{0.5,d}$ = 0.094081329: the branch (red) and its components (blue) (**a**); the branches (red) vs. the M_d set of points (blue) (**b**).

As stated at the beginning of CS1, the DELL laptop represents a consumer of class $k = 1$ and the LCD TV a consumer of class $k = 2$. However, the parameters (B5) and (B6) correspond to a pair of consumers of classes $k = 2$ and $k = 4$. The situation is explained by the fact that class signatures $k = 4$ may often substitute, with negligible errors, signatures of the tangent or discontinuous tangent types.

Combining the partial results obtained, we note the following result: the 2-m_c corresponds to the pair of signatures $i^1(v)$ and $i^2(v)$ calculated using the Formulas (10a) and (10b).

- Consumer 1:

$$i^1(v) = \begin{cases} 0.8 \cdot S_{2\_a}(v) having (B3) parameters\ for\ the\ ascending\ branch \\ 0.8 \cdot S_{2\_d}(v) having (B5) parameters\ for\ the\ descending\ branch \end{cases} \quad (10a)$$

- Consumer 2:

$$i^2(v) = \begin{cases} 0.2 \cdot S_{4\_a}(v) having (B4) parameters\ for\ the\ ascending\ branch \\ 0.2 \cdot S_{4\_d}(v) having (B6) parameters\ for\ the\ descending\ branch \end{cases} \quad (10b)$$

The graphs of the two signatures are illustrated in Figure 8.

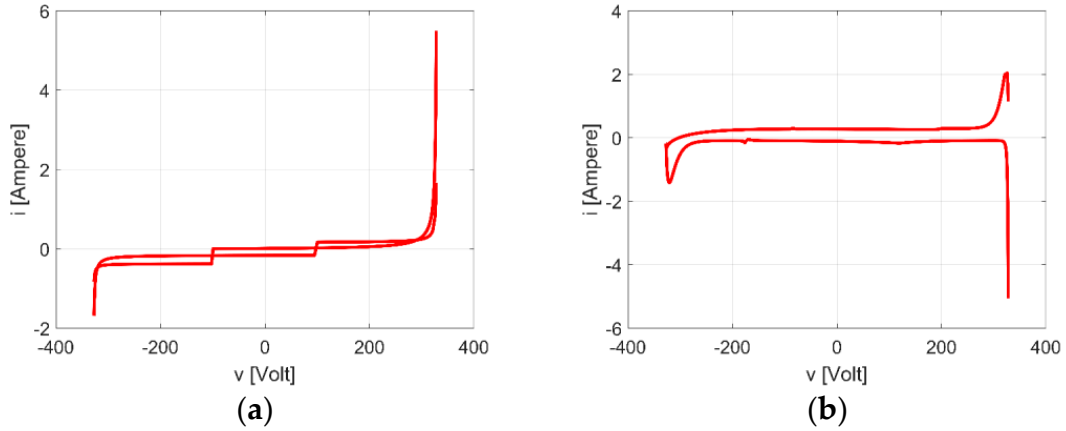

Figure 8. "Pair of simple consumers" solution for 2-m_c in CS 1: the signature of first consumer (**a**); the signature of second consumer (**b**).

4.2. Case Study No. 2

This time, the 2-m_c consists of a vacuum cleaner and an HP laptop with active power levels in a disproportionate ratio of approx. 1/92. The vacuum cleaner is a consumer of class $k = 4$ and the HP laptop a consumer of class $k = 1$ [21]. The point cloud obtained by measurements and the point sets selected for the signature determination (M_a blue and M_d red) are illustrated in Figure 9.

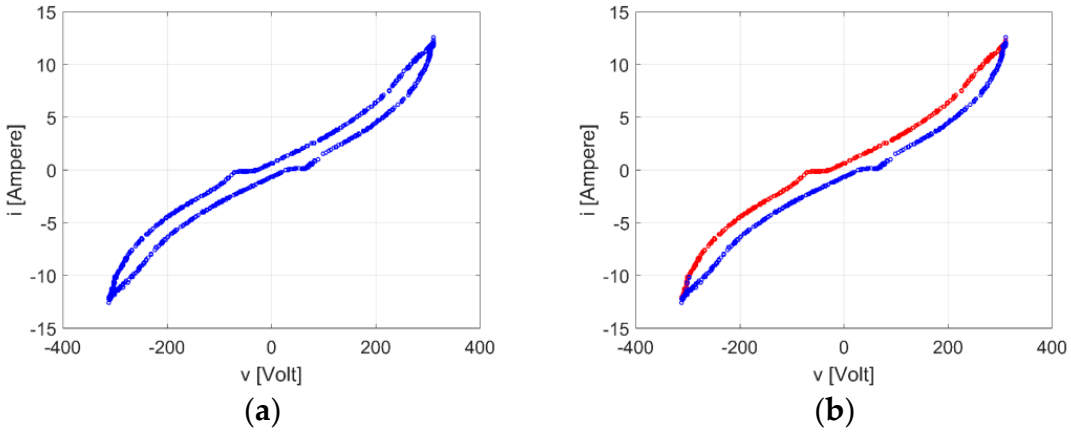

Figure 9. The cloud of measured points (**a**) and the sets of points M_a and M_d (**b**) in CS2.

Under variant 1, it is the fitness in Table 5 that corresponds to the four support functions in Appendix A. The underlined values recommend again the implementation of a simple consumer model of class $k = 4$. The signature has parameters (B7) for the ascending branch and (B8) for the descending branch.

Table 5. The fitness values of the simple equivalent consumers (variant1) in CS2.

r	$k = 1$	$k = 2$	$k = 3$	$k = 4$
a	6.442468	4.79007	1.026761	<u>0.146579</u>
d	6.604708	5.016284	1.084939	<u>0.152357</u>

The branches and signature appear in Figure 10. The M_a and M_d point sets are illustrated in blue and the signatures in red.

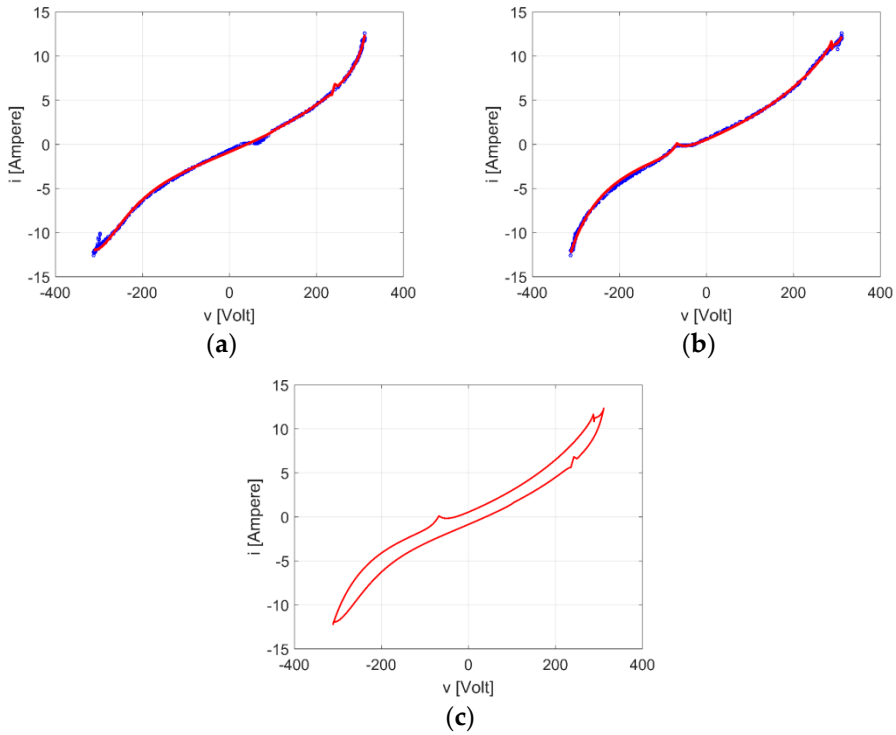

Figure 10. The signature of a *e-s_c* of class $k = 4$ in CS2: the ascending branch (**a**), the descending branch (**b**), the assembly (**c**).

Under variant 3, the results obtained for the 10 combinations $C_{\alpha\beta}$ and the five values of $p \in P$ were not validated for physical reasons. We attribute this to the difference between the powers of the two consumers. As a result, we extended the sequence (4) of the p values with the values 0.015, 0.025, 0.05 and 0.95, 0.975, 0.985, qualitatively close to the values of the power ratios of 1/20, respectively 19/20. Only those parts of the results that are considered relevant for establishing of the signature are included in Table 6.

Table 6. CS2—Maximum frequencies of the analyzed combinations for the *a* and *d* branches and related minimum fitness.

$f_{0.05,a,34} = 0.88$ $F_{0.05,a} = 0.12095$	...	$f_{0.6,a,34} = 0.44$ $F_{0.6,a} = 0.130791518$	...	$f_{0.985,a,44} = 0.4$ $F_{0.985,a} = \underline{0.172632228}$	$(f_{0.6,a,44} = 0.42)$ $(F_{0.6,a,44} = \underline{0.100406146})$
$f_{0.015,d,34} = 0.88$ $F_{0.015,d} = 0.132942854$	...	$f_{0.05,d,34} = 0.82$ $F_{0.05,d} = \underline{0.124737}$	...	$f_{0.5,d,24} = 0.56$ $F_{0.5,d} = 0.094081329$	$f_{0.95,d,44} = 0.39$ $F_{0.95,d} = 0.251224$

Analyzing the signatures in the ascending order of the fitness values in the first row of Table 6, we consider as a viable solution for the ascending branch the one having fitness $F_{0.985,a} = 0.172632228$ corresponding to combination C_{44}. The related signatures are presented in Figure 11. The figure on the left highlights the different size orders of the currents absorbed by the two member consumers. According to the figure on the right, the sum of the current (continuous curve) tracks sufficiently well the measured values except for the current oscillation calculated near the voltage of −100 V. It is due to the approximation of the signature of the consumer of class $k = 1$, the laptop, by a signature of class $k = 4$. The values of the signature parameters of the simple consumers associated with the C_{44} pair are given in (B9) and (B10).

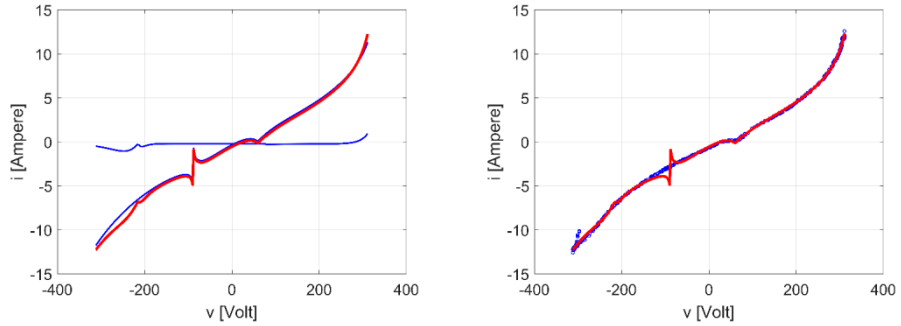

Figure 11. CS2—solution for the ascending branch in variant 3, $F_{0.985,a}$ = 0.172632228: the branch (red) and its components (blue) (**a**); the branch (red) vs. the *Ma* set of points (blue) (**b**).

The minimum fitness on all ascending branches has the value $F_{0.6,a,44}$ = 0.100406146 and occurs for the winning combination, C_{44}, with a frequency $f_{p,a,44}$ = 0.42. The case is indicated in brackets in Table 6. Signatures are presented in Figure 12. They invalidate the mathematical solution that conversed towards a local minimum for which the currents corresponding to the two simple component consumers have the same size range but different polarities.

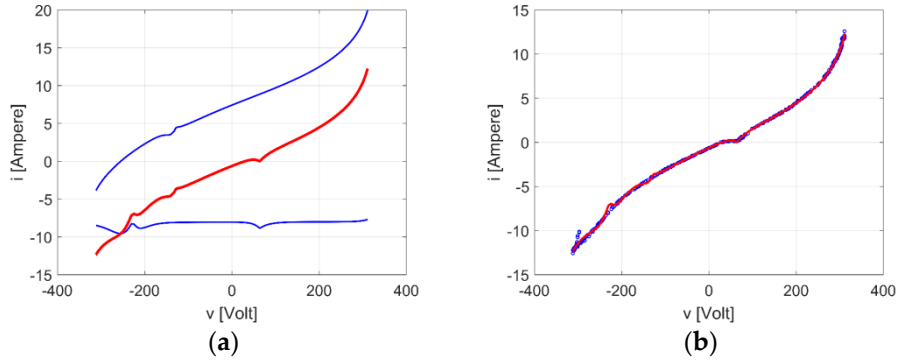

Figure 12. The signatures corresponding to the minimum fitness in CS2, the ascending branch, variant 3, $F_{0.6,a,44}$ = 0.100406146: the branch (red) and its invalid components (blue) (**a**); the branch (red) vs. the *Ma* set of points (blue) (**b**).

For the descending branch the solution is the one with fitness $F_{0.015,d}$ = 0.132942854. It corresponds to p = 0.015 and to the combination C_{34}. The related signatures are presented in Figure 13. In Figure 13a, the consumer of class k = 3 is illustrated by a degenerated ellipse, practically reduced to an axis, and the consumer of class k = 4 by the arch curve specific to this class [21]. The values of the parameters of the simple consumers associated with pair C_{34} are presented in (B11) and (B12). From the point of view of the polarity of currents the solution makes sense physically, but practically the solution does not correspond to the actual situation. On one hand, the current consumed by the consumer of class k = 4 should be much higher than that of the other consumer, on the other hand the right segment should be very slightly sloped to correspond to the actual consumer of class k = 1. However, Figure 13b illustrates a very good match for the aggregate calculated based on the experimental results. This leads to the conclusion that, basically, the simple consumers calculated are relevant in this case only by joint consumption.

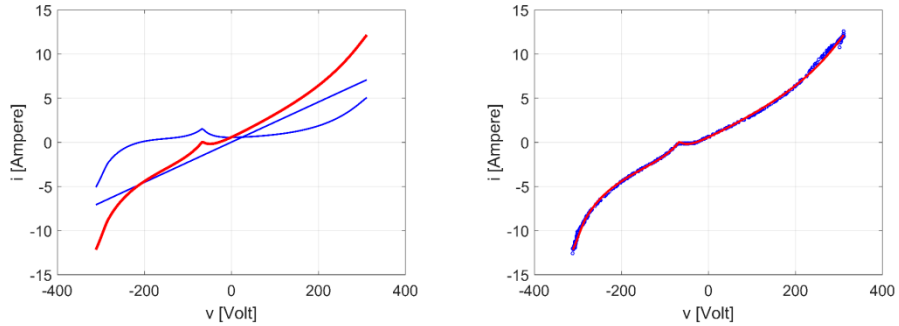

Figure 13. Solution in CS2, descending branch, version 3, $F_{0.015,d} = 0.132942854$: the branch (red) and its components (blue) (**a**); the branch (red) vs. the *Md* set of points (blue) (**b**).

The minimum fitness for the descending branch, $F_{0.05,d} = 0.124737$, has no physical relevance.

Combining the partial results obtained we note the following result: the pair of signatures $i^1(v)$ and $i^2(v)$ calculated with Formulas (11a) and (11b) corresponds to the consumer 2-*m_c*:

- Consumer 1:

$$i^1(v) = \begin{cases} 0.985 \cdot S_{4\_a}(v) having (B9) parameters\ for\ the\ ascending\ branch \\ 0.985 \cdot S_{4\_d}(v) having (B11) parameters\ for\ the\ descending\ branch \end{cases} \quad (11a)$$

- Consumer 2:

$$i^2(v) = \begin{cases} 0.015 \cdot S_{4\_a}(v) having (B10) parameters\ for\ the\ ascending\ branch \\ 0.015 \cdot S_{3\_d}(v) having (B12) parameters\ for\ the\ descending\ branch \end{cases} \quad (11b)$$

The graphs of the two signatures are illustrated in Figure 14.

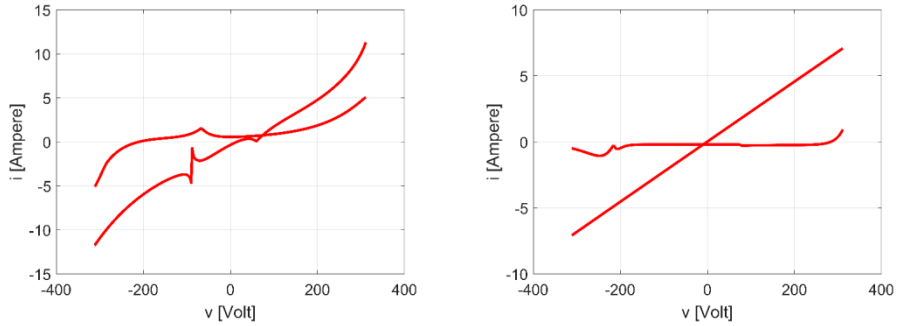

Figure 14. The solution "pair of simple consumers" for the 2-*m.c* in CS2: Consumer 1 (**a**); Consumer 2 (**b**).

4.3. Discussion

In Section 4 we applied the method proposed in Section 3 to two case studie. Our main purpose was to illustrate the way the method can be applied. For the case studies, we chose combinations of consumers with individual signatures known from papers [19,20], as they allowed us to evaluate the new results.

The CS1 and CS2 case studies illustrate that the application of variant 1, i.e., the association of a simple consumer equivalent to a 2-*m_c*, has each time led to a consumer of class $k = 4$. Since, in each case, the signature fitted very well to the $M_a \cup M_d$ point cloud (Figures 3 and 10) the solution was accepted. At the same time, variant 1 is also favorable in terms of the computational volume.

Applying variant 3 raises at least two issues. First, the solutions obtained do not always have a physical equivalent. In Figure 8a the signature cross—hence no physical equivalent, situation that is not observed at ordinary consumers of classes *K*. Instead, the signature in Figure 8b has a physical equivalent, apart from a parasitic line at high positive voltages. On the other hand, in Figure 14 although the branches cross and therefore do not have an expected physical equivalent the combination of the two signatures fits very well on the point cloud $M_a \cup M_d$ (Figure 6, Figure 7, Figure 12, and Figure 13b). This finding suggests that for consumer members of a 2-*m_c*, simple signatures belonging only mathematically to classes *K* should be accepted.

The second issue: it should be noted that the decision validation process for obtaining the signatures of simple consumer members is more laborious, requiring a computing effort and processing capacity which increases with the number of consumers (*n*).

5. Conclusions

The paper shows that for a 2-*m_c*, i.e., for a pair of two consumers connected in parallel, the signatures of type $i(v)$ may be determined on the basis of the processing of the sampled values of the total current and the voltage, measured at a frequency that is lower than that of the voltage of the grid. For this purpose, we present a method which is based on composing the signatures from several types of available support functions using GA. The signature type and its parameters are determined simultaneously.

The paper illustrates two experimental case studies, which aim to investigate the method's ability of composing individual signatures out of global measurements. The conclusions related to the application of the method in these cases, are the following:

The application of the method leads to a single signature equivalent to the consumer pair or a pair of signatures. For both the same consumer power levels and different ones, the method allows the determining of a common equivalent signature. When the power levels of the pair's individual consumers are comparable, the proposed method allows associating of signatures for each consumer separately. Otherwise, pairs of signatures are obtained, which are mathematically equivalent to the consumer pair, but not to each of the individual consumers. Research can be expanded in several directions, primarily by increasing the number of supporting functions and associating common signatures for *n*-*m_c*.

Finally, we must emphasize that the application of the method proposed in this article is not restricted to household consumers, i.e., to the area available to the authors for measurements but can be used in a much wider field.

Author Contributions: Conceptualization, methodology, validation D.-V.C. and T.-L.D.; software, writing—first draft D.-V.C.; writing—review, supervision, and final draft T.-L.D. All authors have read and agreed to the published version of the manuscript.

Funding: This research received no external funding.

Conflicts of Interest: The authors declare no conflict of interest.

Abbreviations

CNN	convolutional neural network
CS1, CS2	case study 1, case study 2
$C_{\alpha\beta}$	pairs of support functions α and β
$C^{\theta}_{\alpha\beta}$	symbol of the $C_{\alpha\beta}$ set from the independent run θ that corresponds to $\min\{F_{\alpha\beta\_r\_p\_\theta}\}_{\alpha\beta \in \{11, \ldots, 44\}}$
e-s_c	equivalent single consumer
$F_{\alpha\beta\_r\_p}$	minimum fitness corresponding to the $C_{\alpha\beta}$ pair of weight p on branch r
$F_{\alpha\beta\_r\_p\_\theta}$	fitness corresponding to the $C_{\alpha\beta}$ pair of weight p on branch r during independent run θ
F_r	the minimum fitness from $F_{p,r}$ set of values, $p \in P$
$F_{p,r}$	fitness corresponding to weight p of branch r

f_{p,r_max}	maximum score
$f_{p,r,\alpha\beta}$	frequency for $C_{\alpha\beta}$ of weight p on branch r and m independent runes
GA	genetic algorithm
$i(v)$	dependence between the voltage v at the consumer's terminals and the absorbed current i
$i^o(v)$	the 'o' dependencies $i(v)$
$i_r^o(v)$	the 'o' trajectory $i(v)$ of branch r
$i(t)$	the value of the current i taken at the discrete-time t
i_j	the measured value of the total absorbed current corresponding to the v_j value of the terminal voltage at the instant t_j
$i_{\alpha\beta\_r\_p}(v)$	total current absorbed by the composed class $\alpha\beta$, of weight p for the branch r
K	group of four classes, $K = \{1, 2, 3, 4\}$
k	class type, $k \in K$
M_r	cloud of points associated to the branch r
N_r	number of measurements allocated to branch r
n-m_c	n multiple consumer
r	type of branch
P	set of values for the weighting parameter
p	weighting parameter
$S_k(v)$	support function associated to the class k
$S_{k\_r}(v)$	support function associated to the class k and branch r
$v(t)$	the value of the voltage v taken at the discrete-time t
V	attenuation constant of the measured voltage values
v_j	value of the terminal voltage at the instant t_j
$\alpha\beta$	pairs of classes (α, β)
Π_{k_r}	parameters for support function $S_{k,r}$
$\Pi_{k\_r\_p}$	parameters for support functions for $S_{k,r,p}$
$\Pi_{k\_r\_p\_\theta}$	parameters for support functions for $S_{k,r,p}$ for the independent run θ
θ	index of independent run

Appendix A

Formulas of Support Functions for k Classes

The formulas of the support functions S_{k_r} for the four classes, $k \in K$, are given here below. They are followed by several specifications regarding the parameters of these functions.

- $k = 1$ (tangent class): $S_{1\_r} : [-V_{\min}, V_{\max}] \to R$,

$$S_{1\_r}(v) = \left(\frac{1}{a_L} tg\frac{v + d_L}{c_L} - \frac{1}{a_L} tg\frac{d_L}{c_L} + \frac{1}{a_R} tg\frac{d_R}{c_R}\right) \cdot \frac{1 - \operatorname{sgn}(v)}{2} + \frac{1}{a_R} tg\frac{v + d_R}{c_R} \cdot \frac{1 + \operatorname{sgn}(v)}{2} + b \tag{A1}$$

- $k = 2$ (discontinuous tangent class): $S_{2\_r} : [-V_{\min}, V_{\max}] \to R$,

$$S_{2\_r}(v) = \left(\frac{1}{a_L} tg\frac{v + d_L}{c_L} + b_L\right) \cdot \frac{1 - \operatorname{sgn}(v)}{2} + \left(\frac{1}{a_R} tg\frac{v + d_R}{c_R} + b_R\right) \cdot \frac{1 + \operatorname{sgn}(v)}{2} \tag{A2}$$

- $k = 3$ (ellipse class): $S_{3\_r} : [-V_{\min}, V_{\max}] \to R$,

$$\begin{aligned} S_{3\_r}(v) = &\left\{\left[\frac{a^2}{V_{\max}^2} - 1\right] \cdot v \cdot \sqrt{\frac{V_{\max}^2 - b^2}{a^2 - V_{\max}^2}} \pm \frac{b \cdot a}{V_{\max}} \cdot \sqrt{1 - \frac{v^2}{V_{\max}^2}}\right\} \cdot \\ &\left(1 + A \cdot \sin\left(3\pi \cdot \frac{v - V_{\min}}{v - V_{\max}}\right)\right) \cdot \exp\left(\frac{|v|}{k \cdot V_{\max}}\right) \end{aligned} \tag{A3}$$

- $k = 4$ (hybrid class): $S_{4\_r} : [-V_{\min}, V_{\max}] \to R$,

$$S_{4\_r}(v) = \sum_{j=1}^{3}\left[I_j + a_{Lj}\cdot\left|v - V_j\right|^{n_{Lj}}\cdot\left(\operatorname{sgn}\left(v - V_j\right)\right)^{\alpha_{Lj}}\cdot\exp\left(b_{Lj}\cdot\left(v - V_j\right)\right)\cdot\frac{1-\operatorname{sgn}\left(v-V_j\right)}{2}\right]+$$

$$\sum_{j=1}^{3}\left[a_{Rj}\cdot\left|v - V_j\right|^{n_{Rj}}\cdot\left(\operatorname{sgn}\left(v - V_j\right)\right)^{\alpha_{Rj}}\cdot\exp\left(b_{Rj}\cdot\left(v - V_j\right)\right)\cdot\frac{1+\operatorname{sgn}\left(v-V_j\right)}{2}\right] + k\cdot f_c(V_x) \quad \text{(A4)}$$

$$f_c(v) = \exp(-[k_1(1-\operatorname{sgn}(v - V_x)) + k_2(1+\operatorname{sgn}(v - V_x))]\cdot|v - V_x|)$$

The capital letters L, R used as indexes (subscript) of parameters, are referring to the "left" side, "right side", respectively, of the r branch of the signature, $r \in \{a, d\}$.

$$\text{The function } \operatorname{sgn}(x) = \begin{cases} -1, x < 0 \\ 0, x = 0 \\ 1, x > 0 \end{cases}$$

facilitates the left/right reporting to the point cloud M_r necessary for determining the parameters associated to each branch $r \in \{a, d\}$. The reporting is performed against $v = 0$ (continuity point) for S_{1_r}, in respect to $v_b = -100$ if $r = a$, $v_b = 100$ if $r = b$ (discontinuity point) for S_{2_r}, and $v = V_j$ for S_{4_r}. In the last case, the "left" side is separated from the "right" side by a "central" area.

For $k = 1$ and $k = 2$ meeting the requirement that the function tg(x) be defined for the entire range [V_{min}, V_{max}] requires connecting relations (A5) and accordingly the elimination of two parameters

$$d_L = (-\pi/2 + \varepsilon)\cdot c_L - V_{\min}, d_R = (\pi/2 - \varepsilon)\cdot c_R - V_{\min}, \varepsilon = 0.001.$$

When $k = 3$ the radicals impose the conditions $a > V_{max}$, $b < V_{max}$, and the brackets with sinusoidal function ensure the peanut shape of the ellipse.

Appendix B

Parameters of Signatures in the Case Studies

- CS1—variant 1

$$\begin{aligned}\Pi_{4,a} = [&-330, -140.418355, 330, -1.206685841, 0.420320105, -0.047258484,\\ &-0.035609074, 1.202484554, -0.308513557, 0.144248474, 0.022806082, 0.03651306, -0.022899695,\\ &-0.124626143, 0.099514774, 1, 1.295577435, 2, 1, 1.754189568, 2, 0.888655841, 52.78957927,\\ &0.999859037, 0.917880807, -1.397708597, 4.148622171, 0.157619968, 1.761067898,\\ &-2.122670194, -0.080660196, 5.385459126] \quad (k = 4)\end{aligned} \quad \text{(A5)}$$

$$\begin{aligned}\Pi_{4,d} = [&-330, 118.9286638, 330, -0.361468852, 0.688502883, -0.200663323, -0.148512041,\\ &0.097511698, -2.511626743, 0.092887626, 0.122748098, 0.027469001, -0.022117557,\\ &-0.005939762, 0.188169526, 1, 1.414210761, 2, 1, 1.702698216, 2, 1.103277381, -82.01830691,\\ &0.488170417, 0.999998666, 0.528450253, -8.335119225, -0.203313011, 3.217395098,\\ &-1.200149619, 0.318271017, 2.24209737] \quad (k = 4)\end{aligned} \quad \text{(A6)}$$

- CS1—variant 3—ascending branch

$$\prod\nolimits_{2,a,0.8} = \{556.03, -0.47, 534.11, 50.03, -0.02, 585.43\}, \quad (k = 2) \quad \text{(A7)}$$

$$\begin{aligned}\prod\nolimits_{4,a,0.2} = \{&-330.00, -172.97, 330.00, -0.56, -2.82, -1.91, -0.28, 0.33, -0.10, -0.12, -0.09, 0.20, -0.18,\\ &-0.18, 0.19, 1.00, 1.83, 2.00, 1.00, 1.94, 2.00, 0.58, 119.96, 0.01, 0.01, -0.42, 0.20, -11.59, -188.84,\\ &31.90, 0.22, 16.14\}, \quad (k = 4)\end{aligned} \quad \text{(A8)}$$

- CS1—variant 3—descending branch

$$\prod\nolimits_{2,d,0.8} = \{227.51, -0.20, 742.48, 73.12, 0.20, 229.12\} \quad (k = 2) \quad \text{(A9)}$$

$$\begin{aligned}\prod\nolimits_{4,d,0.2} = \{&-330.00, 196.48, 330.00, -2.86, 0.30, -0.50, -0.18, -2.71, -0.02, 0.15, 0.01, 0.18, -0.02,\\ &0.11, -0.18, 1.00, 1.99, 2.00, 1.00, 1.86, 2.00, 2.45, -82.91, 0.73, 0.98, 2.04, 3.39, -0.08, -36.24,\\ &-3.95, 3.72, -6.12\} \quad (k = 4)\end{aligned} \quad \text{(A10)}$$

- CS2—variant 1

$$\begin{aligned}\Pi_{4,a} = \{&-330, 241.6747542, 330, -0.587658861, -1.335209714, -0.095339404, -0.013298896,\\ &-1.463871148, -1.714191146, 0.096798825, -0.017791487, 0.001821, -0.030286295,\\ &0.113605457, 0.066772382, 1, 1.061342863, 2, 1, 1.788367122, 2, -9.623733523, 103.2716657,\\ &0.115437276, 0.001643849, 0.099998635, 0.694929314, 3.729717528, 28.52497626,\\ &14.94561319, 0.228573833, 2.590349053\}, \quad (k = 4)\end{aligned} \tag{A11}$$

$$\begin{aligned}\Pi_{4,d} = \{&-330, 288.4559656, 330, -0.69835913, -0.111541204, -0.059074186, -0.060037092,\\ &0.244307797, -0.808240641, 0.097372815, 0.002130477, 0.002945137, -0.013426992,\\ &-0.13397473, 0.067751534, 1, 1.770772699, 2, 1, 1.202506319, 2, -5.866176442, -68.15071066,\\ &0.038127945, 0.029464038, 0.999167982, 7.435667219, 1.638719605, 22.66760565,\\ &-13.52942425, 1.019871112, 8.475106618\}, \quad (k = 4)\end{aligned} \tag{A12}$$

- CS2—variant 3—ascending branch

$$\begin{aligned}\prod_{4,a,0.985} = \{&-330, -88.45682442, 330, -0.886627393, -0.1605959, -0.139920452, -2.961244482,\\ &0.331960325, -0.606538542, -0.126281126, -0.007081717, 0.003747776, -0.193727474,\\ &-0.016503071, 0.06101668, 1, 1.495258987, 2, 1, 1.645819353, 2, -1.644319602, 59.60375292,\\ &0.025791006, 0.012781753, -1.18456939, 2.397929641, 5.387719145, 21.4033764,\\ &-0.005029314, -1.313289822, 0.949587649\}, \quad t(k = 4)\end{aligned} \tag{A13}$$

$$\begin{aligned}\prod_{4,a,0.015} = \{&-330, -214.8841888, 330, -0.187740679, 1.266305623, -0.002663143, -2.988015647,\\ &0.917751051, -0.241920167, -0.004266573, 0.038148773, 0.058082053, -0.191262526,\\ &-0.118784223, 0.185899854, 1, 1.272896179, 2, 1.601771352, 2, -13.6482072, 77.98802887,\\ &0.325548382, 0.00302769, -4.998870972, 3.539275922, 2.387108621, 234.9170775,\\ &-0.00297658, -8.712786589, -4.671751987\}, \quad (k = 4)\end{aligned} \tag{A14}$$

- CS2—variant 3—descending branch

$$\prod_{3,d,0.015} = \{617.5344397, 1.001820073, 1.73558E-05, 49.99807013\}, \quad (k = 3) \tag{A15}$$

$$\begin{aligned}\prod_{4,d,0.985} = \{&-330, -281.0068316, 330, -0.422513103, 1.468095482, -0.621639412, -1.525593683,\\ &0.940312772, -0.007492236, 0.08659972, 0.015285928, -0.006155645, 0.013493475,\\ &-0.012187864, 0.168646641, 1, 1.597097378, 2, 1, 1.812436858, 2, 0.786945874, -66.86886724,\\ &0.017088726, 0.025757337, 1.149448916, -1.052872026, -0.027335466, -3.787297011,\\ &17.05746886, 0.056786824, 8.421205757\}, \quad (k = 4).\end{aligned} \tag{A16}$$

References

1. Paredes-Valverde, M.A.; Alor-Hernández, G.; García-Alcaráz, J.L.; Salas-Zárate, M.P.; Colombo-Mendoza, L.O.; Sánchez-Cervantes, J.L. IntelliHome: An internet of things-based system for electrical energy saving in smart home environment. *Comput. Intell.* **2020**, *36*, 203–224. [CrossRef]
2. Ju, C.; Wang, P.; Goeland, L.; Xu, Y. A Two-Layer Energy Management System for Microgrids With Hybrid Energy Storage Considering Degradation Costs. *IEEE Trans. Smart Grid* **2018**, *9*, 6047–6057. [CrossRef]
3. Geng, L.; Wei, Y.; Lu, Z.; Yang, Y. A novel model for home energy management system based on Internet of Things. In Proceedings of the 2016 IEEE International Conference on Power and Renewable Energy (ICPRE 2016), Shanghai, China, 21–23 October 2016; pp. 474–480. [CrossRef]
4. Rashid, H.; Stankovic, V.; Stankovicand, L.; Singh, P. Evaluation of Nonintrusive Load Monitoring Algorithms for Appliance-level Anomaly Detection. In Proceedings of the 2019 IEEE International Conference on Acoustics, Speech and Signal Processing (ICASSP 2019), Brighton, UK, 12–17 May 2019; pp. 8325–8329. [CrossRef]
5. Ahmad, T.; Chen, H.; Wang, J.; Guo, Y. Review of various modeling techniques for the detection of electricity theft in smart grid environment. *Renew. Sust. Energ. Rev.* **2018**, *82*, 2916–2933. [CrossRef]
6. Hart, G.W. Nonintrusive appliance load monitoring. *Proc. IEEE* **1992**, *80*, 1870–1891. [CrossRef]
7. Lam, H.Y.; Fungand, G.S.K.; Lee, W.K. A Novel Method to Construct Taxonomy Electrical Appliances Based on Load Signatures. *IEEE Trans. Consum. Electron.* **2007**, *53*, 653–660. [CrossRef]
8. Hassan, T.; Javedand, F.; Arshad, N. An Empirical Investigation of V-I Trajectory Based Load Signatures for Non-Intrusive Load Monitoring. *IEEE Trans. Smart Grid* **2014**, *5*, 870–878. [CrossRef]

9. Longjun Wang, A.; Xiaomin Chen, B.; Gang Wang, C.; Hua, D. Non-intrusive load monitoring algorithm based on features of V-I trajectory. *Electr. Power Syst. Res.* **2018**, *157*, 134–144. [CrossRef]
10. Iksan, N.; Sembiring, J.; Haryantoand, N.; Supangkat, S.H. Appliances identification method of non-intrusive load monitoring based on load signature of V-I trajectory. In Proceedings of the 2015 International Conference on Information Technology Systems and Innovation (ICITSI 2015), Bandung, Indonesia, 16–17 November 2015; pp. 1–6. [CrossRef]
11. Du, L.; He, D.; Harleyand, R.G.; Habetler, T.G. Electric Load Classification by Binary Voltage–Current Trajectory Mapping. *IEEE Trans. Smart Grid* **2016**, *7*, 358–365. [CrossRef]
12. De Baets, L.; Ruyssinck, J.; Develder, C.; Dhaene, T.; Deschrijver, D. Appliance classification using VI trajectories and convolutional neural networks. *Energy Build.* **2018**, *158*, 32–36. [CrossRef]
13. De Baets, L.; Develder, C.; Dhaene, T.; Deschrijver, D. Detection of unidentified appliances in non-intrusive load monitoring using siamese neural networks. *Int. J. Electr. Power Energy Syst.* **2019**, *104*, 645–653. [CrossRef]
14. Faustine, A.; Pereira, L. Improved Appliance Classification in Non-Intrusive Load Monitoring Using Weighted Recurrence Graph and Convolutional Neural Networks. *Energies* **2020**, *13*, 3374. [CrossRef]
15. Faustine, A.; Pereira, L. Multi-Label Learning for Appliance Recognition in NILM Using Fryze-Current Decomposition and Convolutional Neural Network. *Energies* **2020**, *13*, 4154. [CrossRef]
16. Baptista, D.; Mostafa, S.S.; Pereira, L.; Sousa, L.; Morgado-Dias, F. Implementation Strategy of Convolution Neural Networks on Field Programmable Gate Arrays for Appliance Classification Using the Voltage and Current (V-I) Trajectory. *Energies* **2018**, *11*, 2460. [CrossRef]
17. Yang, C.C.; Soh, C.S.; Yap, V.V. A systematic approach in load disaggregation utilizing a multi-stage classification algorithm for consumer electrical appliances classification. *Front. Energy* **2019**, *13*, 386–398. [CrossRef]
18. Liu, Y.; Wang, X.; You, W. Non-Intrusive Load Monitoring by Voltage–Current Trajectory Enabled Transfer Learning. *IEEE Trans. Smart Grid* **2019**, *10*, 5609–5619. [CrossRef]
19. Căiman, D.V.; Dragomir, T.L. Nonintrusive load monitoring: Analytic expressions as load signature. In Proceedings of the IEEE 12th International Symposium on Applied Computational Intelligence and Informatics (SACI 2018), Timisoara, Romania, 17–19 May 2018; pp. 15–20. [CrossRef]
20. Căiman, D.V.; Dragomir, T.L. Two voltage-current load signature classes for residential consumers. In Proceedings of the 22nd International Conference on System Theory, Control and Computing (ICSTCC 2018), Sinaia, Romania, 12–14 October 2018; pp. 176–181. [CrossRef]
21. Căiman, D.V.; Dragomir, T.L. Empirical Voltage-current Signatures for Individual Household Consumers Obtained by Non-linear Regression. *Stud. Inform. Control.* **2019**, *28*, 201–212. [CrossRef]